



**HAL**  
open science

## Field statistics in nonlinear composites. II. Applications

Martin Idiart, Pedro Ponte Castañeda

► **To cite this version:**

Martin Idiart, Pedro Ponte Castañeda. Field statistics in nonlinear composites. II. Applications. Proceedings of the Royal Society A: Mathematical, Physical and Engineering Sciences, 2007, 463, pp.203-222. 10.1098/rspa.2006.1757 . hal-00311888

**HAL Id: hal-00311888**

**<https://hal.science/hal-00311888v1>**

Submitted on 28 Aug 2018

**HAL** is a multi-disciplinary open access archive for the deposit and dissemination of scientific research documents, whether they are published or not. The documents may come from teaching and research institutions in France or abroad, or from public or private research centers.

L'archive ouverte pluridisciplinaire **HAL**, est destinée au dépôt et à la diffusion de documents scientifiques de niveau recherche, publiés ou non, émanant des établissements d'enseignement et de recherche français ou étrangers, des laboratoires publics ou privés.

# Field statistics in nonlinear composites.

## II. Applications

BY MARTÍN I. IDIART<sup>1,2</sup> AND PEDRO PONTE CASTAÑEDA<sup>1,2,\*</sup>

<sup>1</sup>*Department of Mechanical Engineering and Applied Mechanics, University of Pennsylvania, Philadelphia, PA 19104-6315, USA*

<sup>2</sup>*Laboratoire de Mécanique des Solides, C.N.R.S. UMR 7649, Département de Mécanique, École Polytechnique, 91128 Palaiseau Cedex, France*

Part I of this work provided a methodology for extracting the statistics of the local fields in nonlinear composites, from the effective potential of suitably perturbed composites. In particular, exact relations were given for the first and even moments of the fields in each constituent phase. In this part, use is made of these exact relations in the context of the ‘variational’, ‘tangent second-order’ and ‘second-order’ nonlinear homogenization methods to generate estimates for the phase averages and second moments of the fields for two-phase, power-law composites with isotropic and transversely isotropic microstructures. The accuracy of these estimates is assessed by confronting them against corresponding exact results for sequentially laminated composites. Among the nonlinear homogenization estimates considered in this work, the second-order estimates are found to be, in general, the most accurate, especially for large heterogeneity contrast and nonlinearity. Thus, these estimates are able to capture, for example, the strong anisotropy in the strain fluctuations that can develop inside nonlinear porous and rigidly reinforced composites.

**Keywords: nonlinear homogenization; variational methods; field fluctuations**

---

### 1. Introduction

In part I of this work (Idiart & Ponte Castañeda in press), we presented a means for extracting the statistics of the local fields in *nonlinear* composites, from the effective potential of suitably perturbed composites. More precisely, the idea is to perturb the local potentials by adding a term that contains a parameter, generally a tensor, such that the derivative of the perturbed effective potential with respect to that parameter, evaluated at the parameter equal to zero, yields the average of the desired quantity in the unperturbed problem. The usefulness of the resulting relations is that they allow the determination of rigorous homogenization estimates for the field statistics, from corresponding estimates for the effective potentials. Such relations were used in part I in the context of the so-called variational, tangent second-order and second-order nonlinear homogenization methods (Ponte Castañeda 1991, 1996, 2002a) to generate estimates

\* Author for correspondence (ponte@seas.upenn.edu).

for the phase averages and second moments of the local fields. It is recalled that these methods are based on suitably designed variational principles making use of ‘optimally’ chosen, fictitious *linear comparison composites* (LCCs), which can be homogenized using any appropriate linear homogenization estimate, so that corresponding estimates are then generated for the effective behaviour of the nonlinear composites.

Recently, several works have been concerned with the use of these nonlinear homogenization methods to estimate the field fluctuations, i.e. higher-order field statistics, in nonlinear *random* composites. Following Ponte Castañeda (2002*b*), Idiart & Ponte Castañeda (2003) first made use of the second-order homogenization method to generate estimates for the field fluctuations in two-phase composites with ‘particulate’ microstructures. Field fluctuations in this class of composites were also studied by Moulinec & Suquet (2003, 2004), by means of the earlier variational homogenization method and full-field numerical simulations. More recently, Idiart *et al.* (2006) have provided comparisons between these numerical simulations and the more sophisticated tangent second-order and second-order methods. Similar studies have also been carried out by Lebensohn *et al.* (2004*a,b*) and Liu & Ponte Castañeda (2004*a,b*) for two- and three-dimensional viscoplastic polycrystals. Brenner *et al.* (2004) also studied field statistics in viscoplastic polycrystals by means of the ‘affine’ method, which is a simplified, but less accurate version of the tangent second-order method, as well as the ‘classical secant’ approach, which is also known to become rather inaccurate at high nonlinearity. In all these works, the homogenization estimates for the field statistics were obtained by making use of various *ad hoc* assumptions based on the conjecture that the first and second moments of the local fields in the relevant LCC constitute reasonable approximations for the corresponding nonlinear quantities. However, it has been shown in part I, by means of the rigorous procedure described in the previous paragraph, that this conjecture is valid only in the context of the variational method, but not in the context of the tangent second order and second-order methods, where ‘correction’ terms arise due to the lack of full stationarity of the relevant functionals with respect to the properties of the LCC. Here, the more consistent homogenization estimates proposed in part I for the field statistics are determined for the specific case of two-phase, power-law random composites with isotropic and transversely isotropic microstructures, and their accuracy is assessed by comparing them with exact results available from the literature (deBotton & Hariton 2002).

## 2. Application to two-phase, power-law composites

In this work, the focus will be on two-phase composites with *random* particulate microstructures, with clearly defined (1) ‘matrix’ and (2) ‘inclusion’ phases. Both phases are assumed to be isotropic, incompressible materials characterized by power-law potentials of the form

$$\phi^{(r)}(\varepsilon_e) = \frac{\varepsilon_0 \sigma_0^{(r)}}{1+m} \left( \frac{\varepsilon_e}{\varepsilon_0} \right)^{1+m}, \quad \psi^{(r)}(\sigma_e) = \frac{\varepsilon_0 \sigma_0^{(r)}}{1+n} \left( \frac{\sigma_e}{\sigma_0^{(r)}} \right)^{1+n}, \quad (2.1)$$

where  $m=1/n$  is the strain-rate sensitivity, such that  $0 \leq m \leq 1$ ,  $\sigma_0^{(r)}$  is the flow stress of phase  $r$ , and  $\varepsilon_0$  is a reference strain. Note that the limiting values,  $m=1$  and  $m=0$ , correspond to linear and rigid-ideally plastic behaviours, respectively. For simplicity, both phases are assumed to have the same exponent  $m$  and reference strain  $\varepsilon_0$ . Then, from the homogeneity of the local potentials (2.1), it follows that the effective potentials can be written as

$$\tilde{W}(\bar{\varepsilon}) = \frac{\varepsilon_0 \tilde{\sigma}_0}{1+m} \left( \frac{\bar{\varepsilon}_e}{\varepsilon_0} \right)^{1+m}, \quad \tilde{U}(\bar{\sigma}) = \frac{\varepsilon_0 \tilde{\sigma}_0}{1+n} \left( \frac{\bar{\sigma}_e}{\tilde{\sigma}_0} \right)^{1+n}, \quad (2.2)$$

where  $\tilde{\sigma}_0$  is the *effective flow stress* of the composite, and  $\bar{\varepsilon}_e$  and  $\bar{\sigma}_e$  are the equivalent macroscopic strain and stress.

Two different classes of composites are considered in this work. The first one corresponds to fibrous composites with transversely isotropic microstructures, subjected to isochoric in-plane loadings. In this case, the effective flow stress  $\tilde{\sigma}_0$  is a function of the strain-rate sensitivity, the heterogeneity contrast and the inclusion concentration. The second one corresponds to isotropic composites, in which case the flow stress  $\tilde{\sigma}_0$  exhibits additional dependence on the macroscopic strain invariant  $\theta$ , defined by  $\cos(3\theta) = 4 \det(\bar{\varepsilon}_d/\bar{\varepsilon}_e)$  (Ponte Castañeda 1996).

In order to analyse the statistics of the local fields in these composites, it is convenient to identify two ‘components’ of the deviatoric strain (resp. stress) tensor which represents its projections ‘parallel’,  $\varepsilon_{\parallel}$  (resp.  $\sigma_{\parallel}$ ) and ‘perpendicular’,  $\varepsilon_{\perp}$  (resp.  $\sigma_{\perp}$ ), to the macroscopic strain (resp. stress). These components can be determined (up to a sign) by the two orthogonal fourth-order projection tensors  $\mathbf{E}$  and  $\mathbf{F}$  as given by expressions (4.52) of part I with  $\check{\varepsilon}^{(r)} = \bar{\varepsilon}$ , through the following relations:  $\varepsilon_{\parallel}^2 = (2/3) (\boldsymbol{\varepsilon} \cdot \mathbf{E} \boldsymbol{\varepsilon})$ ,  $\varepsilon_{\perp}^2 = (2/3) (\boldsymbol{\varepsilon} \cdot \mathbf{F} \boldsymbol{\varepsilon})$ ,  $\sigma_{\parallel}^2 = (3/2) (\boldsymbol{\sigma} \cdot \mathbf{E} \boldsymbol{\sigma})$  and  $\sigma_{\perp}^2 = (3/2) (\boldsymbol{\sigma} \cdot \mathbf{F} \boldsymbol{\sigma})$ . They are such that  $\varepsilon_e^2 = \varepsilon_{\parallel}^2 + \varepsilon_{\perp}^2$  and  $\sigma_e^2 = \sigma_{\parallel}^2 + \sigma_{\perp}^2$ . In addition, it can be shown that the strain and stress fields are homogeneous of degree one in  $\bar{\varepsilon}_e$  and  $\bar{\sigma}_e$ , respectively, so that normalized quantities such as  $(\varepsilon_e^{(r)}/\bar{\varepsilon}_e)$  and  $(\sigma_e^{(r)}/\bar{\sigma}_e)$  depend only on material and microstructural parameters, and on  $\theta$ .

The nonlinear homogenization methods described in part I require the use of estimates for the effective behaviour of linear elastic and linear thermoelastic composites with phases characterized by a modulus tensor  $\mathbf{L}_0^{(r)}$ , a ‘thermal stress’  $\boldsymbol{\tau}_0^{(r)}$ , and a ‘specific heat’  $f_0^{(r)}$  (see expression (4.31) in part I). In this work, use is made of the generalized Hashin–Shtrikman (HS) estimates of Willis (1981). For two-phase, linear elastic composites, the effective modulus tensor can be written as  $\tilde{\mathbf{L}}_0 = \mathbf{L}_0^{(1)} \mathbf{A}^{(1)} + \mathbf{L}_0^{(2)} \mathbf{A}^{(2)}$ , where  $\mathbf{A}^{(r)}$  are strain concentration tensors such that  $c^{(1)} \mathbf{A}^{(1)} + c^{(2)} \mathbf{A}^{(2)} = \mathbf{I}$ . Defining  $\Delta \mathbf{L}_0 = \mathbf{L}_0^{(2)} - \mathbf{L}_0^{(1)}$ , the HS estimates for the strain concentration tensor in the inclusion phase  $\mathbf{A}^{(2)}$  can be written as

$$\mathbf{A}^{(2)} = \left[ \mathbf{I} + c^{(1)} \mathbf{P}_0^{(1)} \Delta \mathbf{L}_0 \right]^{-1}. \quad (2.3)$$

In this expression, the microstructural tensor  $\mathbf{P}_0^{(1)}$  is given by

$$\mathbf{P}_0^{(1)} = \frac{1}{4\pi \det \mathbf{Z}} \int_{|\boldsymbol{\xi}|=1} \mathbf{H}^{(1)}(\boldsymbol{\xi}) |\mathbf{Z}^{-1} \boldsymbol{\xi}|^{-3} dS(\boldsymbol{\xi}),$$

where  $H_{ijkl}^{(1)}(\boldsymbol{\xi}) = N_{ik}^{(1)} \xi_j \xi_h |_{(ij)(kh)}$ ,  $\mathbf{N}^{(1)} = \mathbf{K}^{(1)-1}$ ,  $K_{ik}^{(1)} = L_{0_{ijkh}}^{(1)} \xi_j \xi_h$ , and the second-order tensor  $\mathbf{Z}$  serves to characterize the ‘shape’ of the assumed ‘ellipsoidal’ two-point correlation functions, such that  $\mathbf{Z} = \text{diag}(1, 1, 1)$  and  $\mathbf{Z} = \text{diag}(1, 1, 0)$  correspond to isotropic and transversely isotropic microstructures, respectively. For two-phase, linear thermoelastic composites, use can be made of the Levin relations (Levin 1967) to relate the ‘thermo-elastic’ quantities to the purely ‘elastic’ ones by means of standard relations, which will not be included here for conciseness.

These linear HS estimates are known to be quite accurate for particulate random systems like the ones of interest in this work, up to moderate concentrations of inclusions.

In order to assess the accuracy of the nonlinear homogenization estimates, *exact* results have been generated for power-law composites with a special type of particulate microstructures called multiple-rank sequential laminates, following the procedure described in deBotton & Hariton (2002). These authors showed that there are two-dimensional lamination sequences for which the macroscopic behaviour tends to be more transversely isotropic as the rank increases. In fact, making use of a differential scheme as described by deBotton (2005), it can be shown analytically that the macroscopic behaviour of these composites does become transversely isotropic in the limit of infinite rank. Similarly, three-dimensional lamination sequences can also be found so that in the limit of infinite rank, the macroscopic behaviour becomes isotropic (Idiart in preparation). The interest in composites with this class of (transversely) isotropic microstructures is that, in the *linear* case, these reproduce *exactly* the effective behaviour of the above-mentioned HS estimates, for *any* values of the modulus tensors of the phases (Milton 2002). For this reason, homogenization estimates of the HS type, like the ones considered here for the LCC, are particularly appropriate for *nonlinear* composites with this class of microstructures, since the effective behaviour of the LCC is being computed exactly in that case, and therefore there is only one level of approximation involved, namely, at the linearization stage. In addition, since this property holds for any type of linearization scheme, this class of nonlinear composites provide an ideal test case to compare LCC-based homogenization methods by making use of different linearization schemes. Furthermore, a peculiarity of this class of nonlinear composites is that, by construction, the local fields in the inclusion phase are uniform, independently of the behaviour of the phases. In this connection, it is relevant to emphasize that the sequentially laminated microstructures are intrinsically different from the ‘composite cylinder assemblage’ (CCA) microstructures considered by Moulinec & Suquet (2003, 2004) also for two-phase, power-law composites with transversely isotropic symmetry. While these two very different types of microstructures are found to exhibit very similar in-plane behaviours when the phases are linear, their behaviours become progressively more different as the nonlinearity increases, the difference being most notable for the case of an ideally plastic matrix containing weaker inclusions. In this case, the most striking difference is the fact that the strain fluctuations in the inclusion phase are infinite in CCA composites, but identically zero in sequential laminates. As the HS-type nonlinear homogenization estimates are consistent with zero fluctuations in the inclusion phase, in this work, we have chosen to compare these nonlinear estimates with the corresponding (infinite-rank) laminate results, instead of the CCA results, as in Idiart *et al.* (2006).

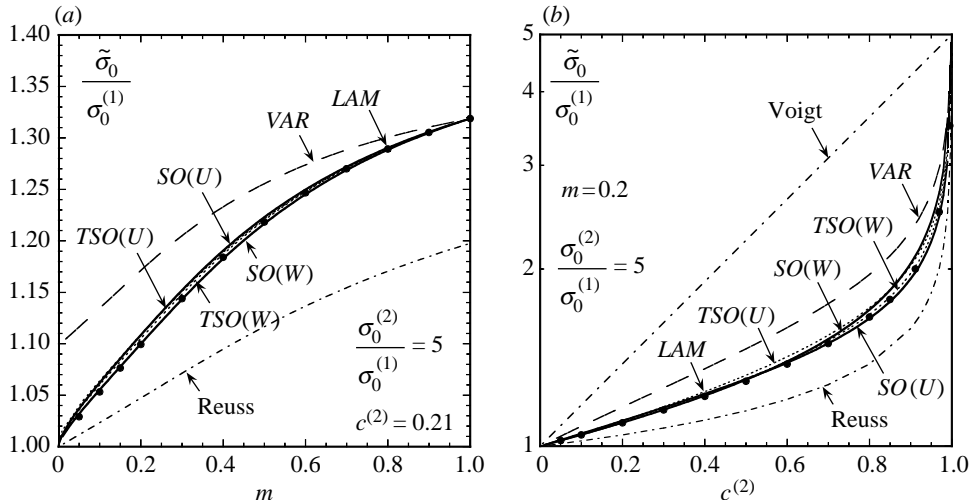


Figure 1. Effective flow stress  $\tilde{\sigma}_0$ , normalized by the flow stress of the matrix  $\sigma_0^{(1)}$ , for power-law, fibre-reinforced ( $\sigma_0^{(2)}/\sigma_0^{(1)}=5$ ) composites subjected to in-plane shear: (a) as a function of the strain-rate sensitivity  $m$ , for a given concentration of fibres ( $c^{(2)}=0.21$ ), (b) as a function of fibre concentration  $c^{(2)}$ , for a given strain-rate sensitivity ( $m=0.2$ ). Comparisons between the ‘second-order’ (SO), ‘tangent second-order’ (TSO) and ‘variational’ (VAR) estimates of the Hashin–Shtrikman type, and exact results for power-law laminates (LAM).

In the sections to follow, comparisons are provided among the exact results for power-law laminates (LAM), and the variational (VAR), tangent second-order (TSO) and second-order (SO) estimates described in part I, for fibre-reinforced ( $\sigma_0^{(2)}/\sigma_0^{(1)}=5$ ) and fibre-weakened ( $\sigma_0^{(2)}/\sigma_0^{(1)}=0.2$ ) composites, as well as for isotropic, rigidly reinforced and porous composites. It is recalled that the SO and TSO estimates exhibit a duality gap, and therefore two sets of these estimates corresponding to the strain (W) and stress (U) formulations are shown. It should also be mentioned that the SO estimates provided in this work make use of  $\bar{\epsilon}$  and  $\bar{\sigma}$  as the ‘reference’ strain and stress tensors (see part I). Finally, the classical bounds of Voigt and Reuss for the effective behaviour are also included for comparison purposes.

### 3. Transversely isotropic, fibre-reinforced composites

#### (a) Effective behaviour

In figure 1, plots are provided for the effective flow stress  $\tilde{\sigma}_0$  of a fibre-reinforced composite, normalized by the flow stress of the matrix phase  $\sigma_0^{(1)}$ . Figure 1a shows plots as a function of the strain-rate sensitivity  $m$ . Several observations are relevant in the context of this figure. First, all homogenization estimates of the HS type coincide for  $m=1$  with the linear HS estimates and the LAM results, but give different predictions for other values of  $m$ . The main observation, however, is that both versions (W and U) of the SO and TSO estimates are in very good agreement with the exact LAM results, for all values of the strain-rate sensitivity  $m$ . In particular, the agreement is excellent for the

$SO(W)$  estimates. In addition, all these estimates are found to tend to the Reuss lower bound as  $m \rightarrow 0$ , which seems to be the case for the  $LAM$  results as well (for numerical reasons, it was not possible to reach  $m=0$ ). The  $VAR$  estimates, on the other hand, are seen to overestimate the  $LAM$  results for all values of  $m$  different from 1, which is not surprising given the fact that the former are known to provide rigorous bounds for the latter. It is also observed that the strain ( $W$ ) and stress ( $U$ ) versions of the  $SO$  and  $TSO$  estimates give slightly different predictions, i.e. they exhibit a duality gap, as anticipated. However, this gap can be shown to vanish not only in the linear case, but also in the ideally plastic limit ( $m=0$ ). Figure 1b shows plots as a function of the fibre concentration for a moderate nonlinearity ( $m=0.2$ ). The main observation is again the good accord of the  $SO$  and  $TSO$  estimates with the  $LAM$  results, even at high-fibre concentrations. It is also interesting to note that the  $SO(W)$  estimates are more accurate than the  $SO(U)$  estimates for low-to-moderate values of  $c^{(2)}$ , while the converse is true for high values of  $c^{(2)}$ .

(b) *First moments of the local fields*

In figure 2, results are given for the corresponding first moments (phase averages) of the local fields. Figure 2a,b shows plots for the equivalent part of the average strains in each phase  $\bar{\varepsilon}_e^{(r)}$ , normalized by the equivalent macroscopic strain  $\bar{\varepsilon}_e$ . It can be seen that all homogenization estimates are in excellent agreement with the  $LAM$  results, for all values of  $m$  and  $c^{(2)}$ . Thus, it is found in figure 2a that the strain in the fibres decreases with increasing nonlinearity (decreasing  $m$ ) until it vanishes in the ideally plastic limit, meaning that the fibres behave like rigid inclusions in this strongly nonlinear limit, even though they are not rigid, and all the macroscopic deformation is carried in the matrix phase. Figure 2b shows that, for a moderate nonlinearity ( $m=0.2$ ), the strain in the fibres remains very small for most values of  $c^{(2)}$ , and hence the average strain in the matrix is  $\bar{\varepsilon}_e^{(1)} \approx \bar{\varepsilon}_e / c^{(1)}$ .

The corresponding results for the average stresses in each phase  $\bar{\sigma}_e^{(r)}$  are shown in figure 2c,d, normalized by the equivalent macroscopic stress  $\bar{\sigma}_e$ . Figure 2c shows plots as a function of  $m$ . Once again, it is seen that the  $SO$  and  $TSO$  estimates are in good agreement with the  $LAM$  results for all values of  $m$ , while the  $VAR$  estimates are rather inaccurate. In particular, the agreement is found to be excellent for the  $SO(W)$  estimates. Thus, these estimates predict a higher average stress in the (stronger) fibres than in the matrix phase, as expected, but as the nonlinearity increases, this difference becomes smaller and finally vanishes as  $m \rightarrow 0$ , so that  $\bar{\sigma}_e^{(1)} = \bar{\sigma}_e^{(2)} = \bar{\sigma}_e$  in this limit. This is consistent with the stress field becoming uniform throughout the composite in the ideally plastic limit, which in turn is consistent with the effective behaviour being given by the Reuss lower bound (see figure 1a). Figure 2d shows that the relative merits of the different homogenization estimates for the average stresses in fact change with fibre concentration. Thus, while the  $SO(W)$  estimates are seen to be the most accurate ones for fibre concentrations below 0.5, they deteriorate significantly at higher concentrations. This deterioration can be traced to the use of  $\bar{\varepsilon}$  as the reference strain, which suggests that this choice is not good for very large concentrations. In contrast, the use of  $\bar{\sigma}$  as the reference stress in the context of the  $SO(U)$  estimates is seen to lead to better behaved, albeit sometimes less accurate, estimates for all values of  $c^{(2)}$ .

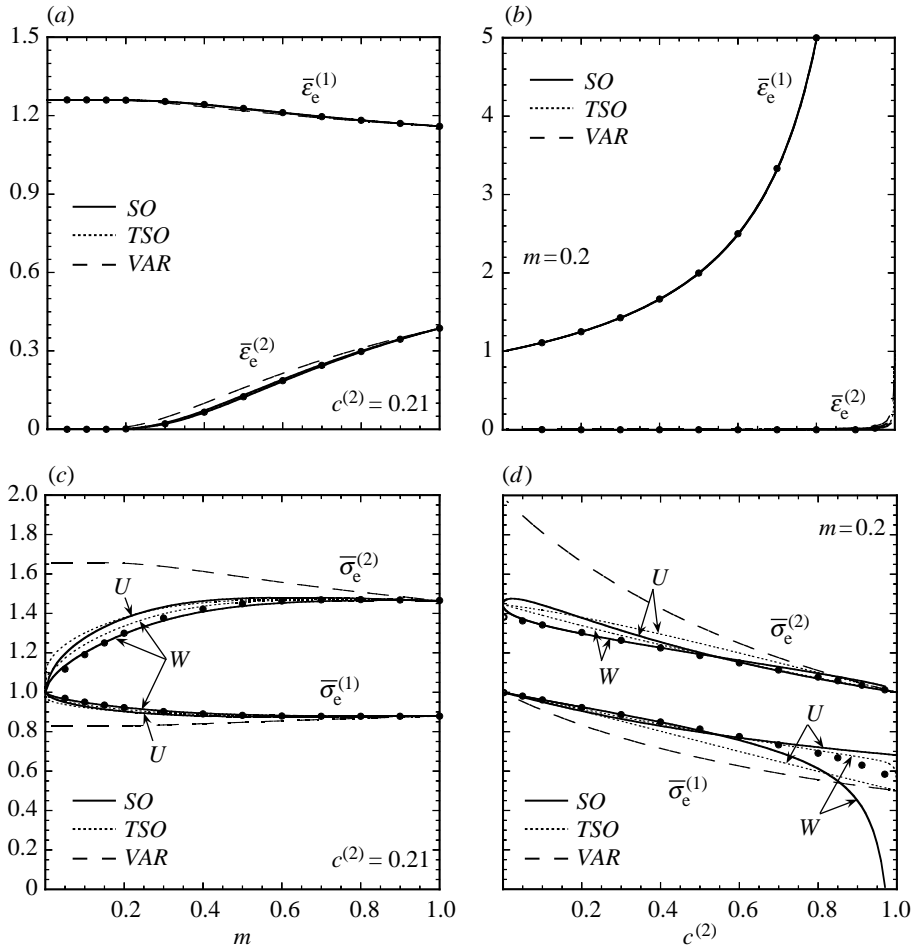


Figure 2. First moments (phase averages) of the local fields in fibre-reinforced composites. Equivalent average strain  $\bar{\varepsilon}_e^{(r)}$  and stress  $\bar{\sigma}_e^{(r)}$  in each phase, normalized by the macroscopic equivalent strain  $\bar{\varepsilon}_e$  and stress  $\bar{\sigma}_e$ , respectively.

### (c) Second moments of the local fields

Plots for the corresponding second moments of the strain field are given in figure 3, normalized by  $\bar{\varepsilon}_e^2$ . Figure 3a shows plots for the second moments of the parallel component of the strain in each phase, as a function of  $m$ . It can be seen in this figure that, in the matrix phase, the *LAM* results increase significantly with increasing nonlinearity, and tend to become unbounded as  $m \rightarrow 0$ , unlike the first moments of the strain, which remain finite in this limit (see figure 2a). This implies that the spatial distribution of the strain in the matrix phase becomes significantly more heterogeneous with increasing nonlinearity. On the other hand, figure 3c shows that the *LAM* results for the second moments of  $\varepsilon_{\perp}$  in the matrix drop to zero as  $m \rightarrow 0$ , meaning that in this limit the strain field becomes ‘aligned’ with the macroscopic strain throughout the composite. In addition, for a finite value of  $m$ , the second moments of both components in the matrix are seen in figure 3b,d to increase monotonically with increasing concentration of fibres, becoming



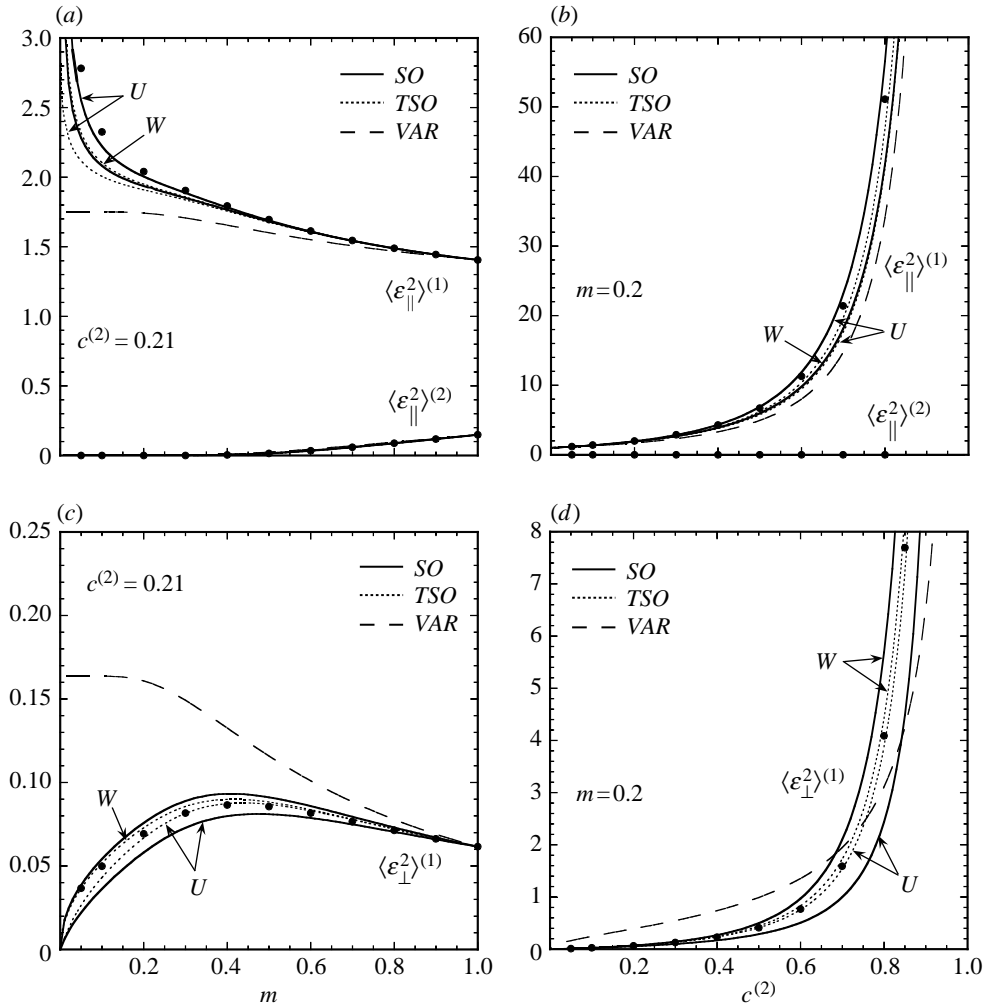


Figure 3. Second moments of the strain field in fibre-reinforced composites. ‘Parallel’  $\varepsilon_{\parallel}$  and ‘perpendicular’  $\varepsilon_{\perp}$  components, normalized by  $\bar{\varepsilon}_e^2$ .

unbounded as  $c^{(2)} \rightarrow 1$ . Both versions of the *SO* and *TSO* estimates are found to be consistent with these observations, being in good qualitative agreement with the *LAM* results for all values of  $m$  and  $c^{(2)}$ . On the other hand, the *VAR* estimates are found, once again, to be the least accurate among the nonlinear homogenization estimates. Finally, it is recalled that the local fields in the *inclusion* phase of the power-law laminates are *uniform* for any value of the material parameters. Thus, the *LAM* results in the inclusion phase are such that  $\bar{\sigma}_e^{(2)}/\sigma_0^{(2)} = (\bar{\varepsilon}_e^{(2)}/\varepsilon_0)^m$ ,  $\langle \varepsilon_{\parallel}^2 \rangle^{(2)} = (\bar{\varepsilon}_e^{(2)})^2$  and  $\langle \varepsilon_{\perp}^2 \rangle^{(2)} = 0$ . In this connection, it is noted that, while the *SO* and *VAR* estimates satisfy these relations, thus being consistent with uniform fields in the fibres, the *TSO* estimates do not satisfy the first two. In fact, the *TSO* estimates for  $\langle \varepsilon_e^2 \rangle^{(2)}$  are found to be slightly less than those for  $(\bar{\varepsilon}_e^{(2)})^2$ , and therefore violate the rigorous inequality  $\langle \varepsilon_e^2 \rangle^{(2)} \geq (\bar{\varepsilon}_e^{(2)})^2$ . This inconsistency demonstrates that the *TSO* estimates are less good than the *SO* estimates.

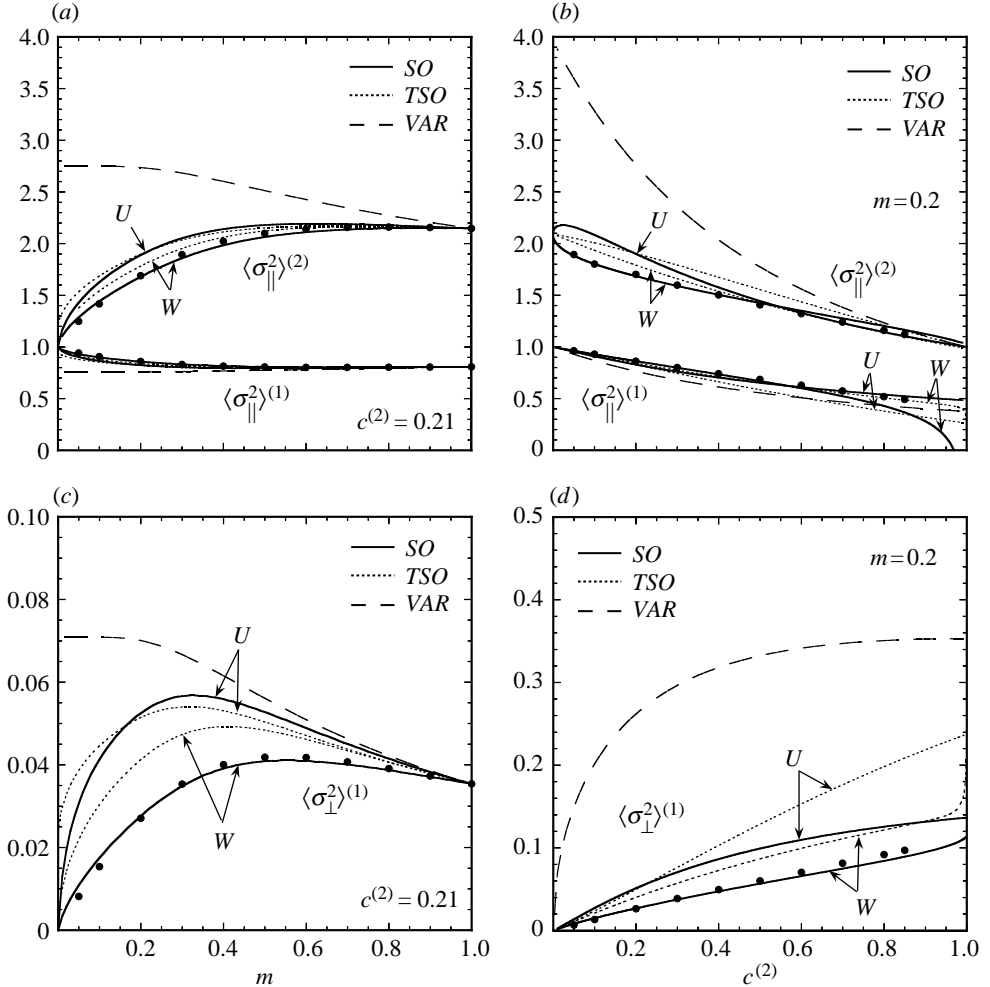


Figure 4. Second moments of the strain field in fibre-reinforced composites. ‘Parallel’  $\sigma_{\parallel}$  and ‘perpendicular’  $\sigma_{\perp}$  components, normalized by  $\bar{\sigma}_e^2$ .

Plots for the corresponding second moments of the parallel  $\sigma_{\parallel}$  and perpendicular  $\sigma_{\perp}$  components of the stress, normalized by  $\bar{\sigma}_e^2$ , are given in figure 4. Figure 4a,c shows plots as a function of  $m$ . The  $LAM$  results show that the second moments of the stress remain bounded as  $m \rightarrow 0$ , unlike those of the strain and seem to be consistent with vanishing fluctuations in the ideally plastic limit. It can be seen that  $SO$  and  $TSO$  estimates are in good qualitative agreement with the  $LAM$  results for all values of  $m$ , and predict no stress fluctuations in the ideally plastic limit, which is consistent with the fact that the corresponding estimates for  $\tilde{\sigma}_0$  attain the Reuss lower bound in this limit. In particular, the agreement is seen to be excellent for the  $SO(W)$  estimates, at least for this moderate value of fibre concentration ( $c^{(2)} = 0.21$ ). Figure 4b,d shows that the  $SO(W)$  estimates remain the most accurate among the homogenization estimates up to fairly large fibre concentrations. However, as  $c^{(2)}$  becomes larger, the  $SO(W)$  estimates for the second moments of  $\sigma_{\parallel}$  in the matrix deteriorate

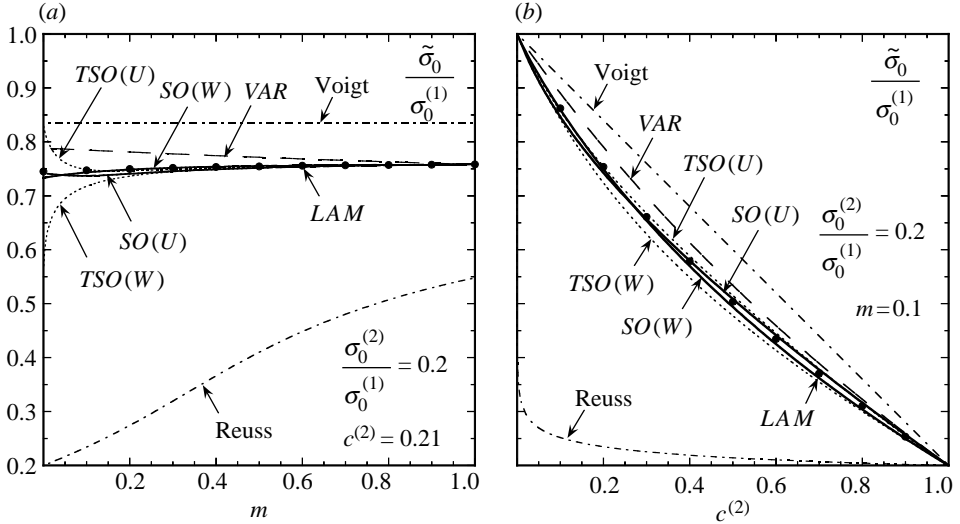


Figure 5. Effective flow stress  $\tilde{\sigma}_0$ , normalized by the flow stress of the matrix  $\sigma_0^{(1)}$ , for power-law, fibre-weakened ( $\sigma_0^{(2)}/\sigma_0^{(1)} = 0.2$ ) composites subjected to in-plane shear: (a) as a function of the strain-rate sensitivity  $m$ , for a given concentration of fibres ( $c^{(2)} = 0.21$ ), (b) as a function of fibre concentration  $c^{(2)}$ , for a given strain-rate sensitivity ( $m = 0.1$ ). Comparisons between the ‘second-order’ ( $SO$ ), ‘tangent second-order’ ( $TSO$ ) and ‘variational’ ( $VAR$ ) estimates of the Hashin–Shtrikman type, and exact results for power-law laminates ( $LAM$ ).

significantly, while the  $SO(U)$  estimates remain well behaved, which is consistent with the observations made in the context of figure 2d. Finally, as already noted in the context of figure 3, it should be mentioned that, while the  $SO$  and  $VAR$  estimates are consistent with uniform fields in the inclusion phase, in agreement with the  $LAM$  results, both versions of the  $TSO$  estimates for the average and second moments of the stress in the inclusion phase are not so and violate the inequality  $\langle \sigma_e^2 \rangle^{(2)} \geq (\bar{\sigma}_e^{(r)})^{(2)}$ . Again, this suggests that the  $TSO$  estimates should be less reliable, in general, than the  $SO$  estimates, as expected.

#### 4. Transversely isotropic, fibre-weakened composites

##### (a) Effective behaviour

In figure 5, plots are provided for the effective flow stress  $\tilde{\sigma}_0$  of a fibre-weakened composite, normalized by the flow stress of the matrix phase  $\sigma_0^{(1)}$ . Figure 5a shows plots as a function of the strain-rate sensitivity  $m$ . The main observation in the context of this figure is that both versions of the  $SO$  estimates are found to be in very good agreement with the  $LAM$  results, not only for weak nonlinearities, but more importantly, also for strong nonlinearities. In contrast, the  $TSO$  estimates are seen to be in very good agreement with the exact  $LAM$  results for weak-to-moderate nonlinearities, but, unlike in the case of stronger fibres, they are seen to deteriorate and deviate significantly from each other (large duality gap) for strong nonlinearities. In this connection, it is observed that, as  $m \rightarrow 0$  the  $TSO(W)$  estimates rapidly decrease to a finite value well

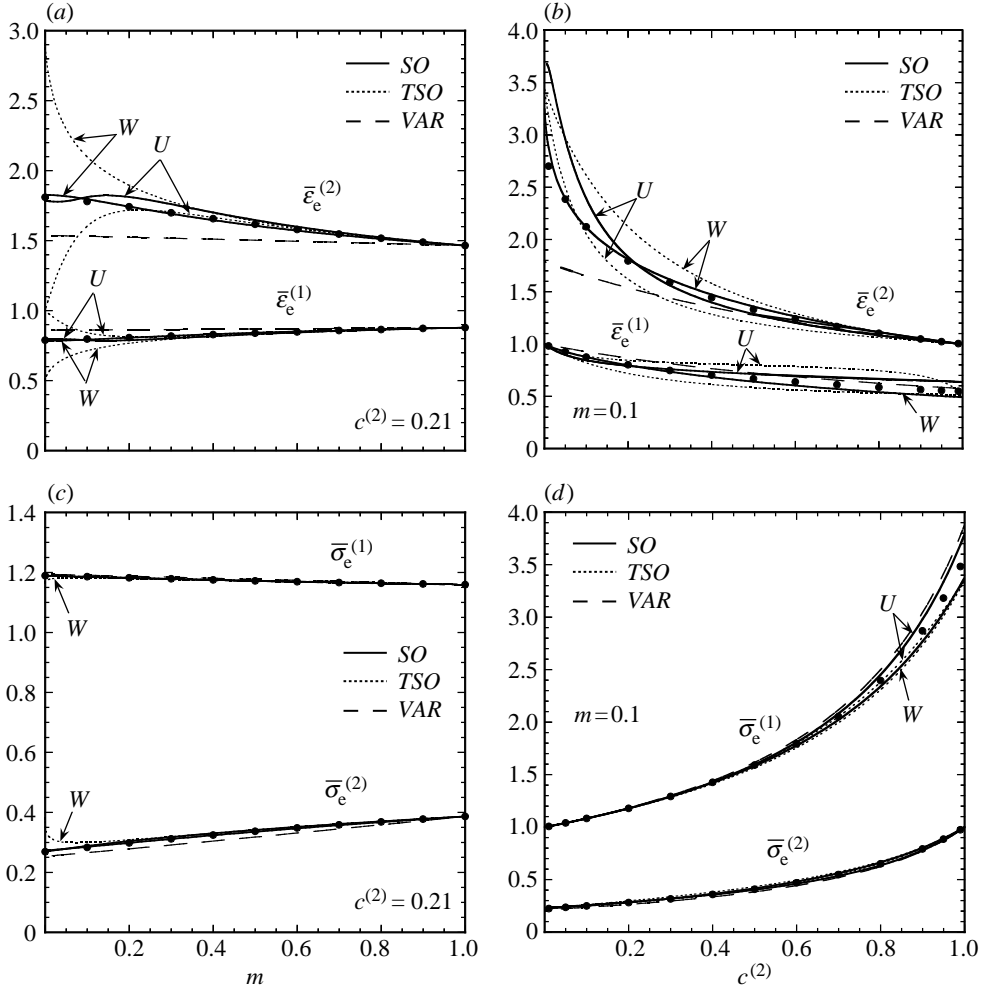


Figure 6. First moments (phase averages) of the local fields in fibre-weakened composites. Equivalent average strain  $\bar{\epsilon}_e^{(r)}$  and stress  $\bar{\sigma}_e^{(r)}$  in each phase, normalized by the macroscopic equivalent strain  $\bar{\epsilon}_e$  and stress  $\bar{\sigma}_e$ , respectively.

below the *LAM* results, while the *TSO(U)* estimates tend to go to the Voigt upper bound, violating the sharper bound provided by the *VAR* estimates. Finally, it can be seen in part (b) that, for a strong nonlinearity ( $m=0.1$ ), the *SO* estimates remain the most accurate for all values of the fibre concentration.

(b) *First moments of the local fields*

Plots for the corresponding phase averages of the local fields are provided in figure 6. Figure 6a shows the equivalent average strains  $\bar{\epsilon}_e^{(r)}$  in each phase, normalized by  $\bar{\epsilon}_e$ , as a function of  $m$ . It can be seen in this figure that the *LAM* results show an average deformation that is higher in the (weaker) fibres than in the matrix, as expected, and that increases with increasing nonlinearity. The *SO(W)* estimates are found to be in excellent agreement with the *LAM* results for

all values of  $m$ , while the agreement is less good for the  $SO(U)$  estimates, which exhibit a peculiar, non-monotonic behaviour close to the ideally plastic limit. On the other hand, the  $TSO$  estimates are in very good agreement with the  $LAM$  results up to moderate nonlinearities, but deteriorate significantly as  $m \rightarrow 0$ . In particular, the  $TSO(U)$  estimates give  $\bar{\varepsilon}_e^{(1)} = \bar{\varepsilon}_e^{(2)} = \bar{\varepsilon}_e$ , which is consistent with the  $TSO(U)$  estimates for  $\bar{\sigma}_0$  being given by the Voigt bound (see figure 5a). Finally, the  $VAR$  estimates are seen to capture the right trends, even if they underestimate significantly the deformation of the inclusion phase for strong nonlinearities. Figure 6b shows that the  $SO(W)$  estimates remain the most accurate for all values of the fibre concentration. These estimates agree with the  $LAM$  results in that the deformation in the inclusion phase increases with decreasing fibre concentrations, and that this trend is significantly enhanced by nonlinearity.

Figure 6c,d shows plots for the equivalent average stresses  $\bar{\sigma}_e^{(r)}$  in each phase. We begin by noting that the  $LAM$  results show an average stress that is lower in the (weaker) fibres than in the matrix, as expected, and that decreases with increasing nonlinearity. The main observation in the context of these figures, however, is that all homogenization estimates are in very good agreement with the  $LAM$  results, for all values of  $m$  and  $c^{(2)}$ . This is not surprising, for in the limit of void fibres ( $\sigma_0^{(2)} = 0$ ) all the estimates predict the correct ratios  $\bar{\sigma}_e^{(r)}/\bar{\sigma}_e$ . However, it is observed in part (c) that, as  $m \rightarrow 0$ , the  $TSO(W)$  estimates exhibit a peculiar behaviour, deviating from the exact  $LAM$  results and thus becoming less accurate than the other estimates in this strongly nonlinear limit.

### (c) Second moments of the local fields

Figure 7 shows plots for the second moments of the parallel  $\varepsilon_{\parallel}$  and perpendicular  $\varepsilon_{\perp}$  components of the strain in each phase, as a function of  $m$  (figure 7a,c) and fibre concentration (figure 7b,d). We begin by noting that the general agreement between the exact  $LAM$  results and the different homogenization estimates is worse than that found for the first moments of the strain (see figure 6a,b). Of all the homogenization estimates, the  $SO(U)$  estimates seem to be the most consistent with the  $LAM$  results, in general, even though they exhibit the peculiar behaviour for strong nonlinearities already observed in the context of figure 6a. On the other hand, while better for the second moments of the strain in the inclusion phase, in the matrix phase the  $SO(W)$  estimates underestimate considerably the second moments of  $\varepsilon_{\perp}$ . However, both versions of the  $SO$  estimates are consistent with uniform fields in the inclusion phase, in agreement with the exact  $LAM$  results. In contrast, both versions of the  $TSO$  estimates are relatively good for weak-to-moderate nonlinearities, but become meaningless for sufficiently strong nonlinearities, violating once again, the rigorous inequality  $\langle \varepsilon_e^2 \rangle^{(r)} \geq (\bar{\varepsilon}_e^{(r)})^2$  in the inclusion phase ( $r=2$ ) and sometimes even in the matrix phase ( $r=1$ ). It should be noted that, in the limit  $m \rightarrow 0$ , the  $TSO(U)$  estimates for  $\bar{U}$  deviate from the Voigt bound when the perturbation parameters  $\lambda^{(r)}$  (see part I) are non-zero, and therefore the  $TSO(U)$  estimates for the second moments of the strain do not agree with uniform strain fields, unlike those for the phase averages.

Figure 8 shows plots for the second moments of the parallel  $\sigma_{\parallel}$  and perpendicular  $\sigma_{\perp}$  components of the stress in each phase, as a function of  $m$  (figure 8a,c) and fibre concentration (figure 8b,d). Once again, it is noted that the

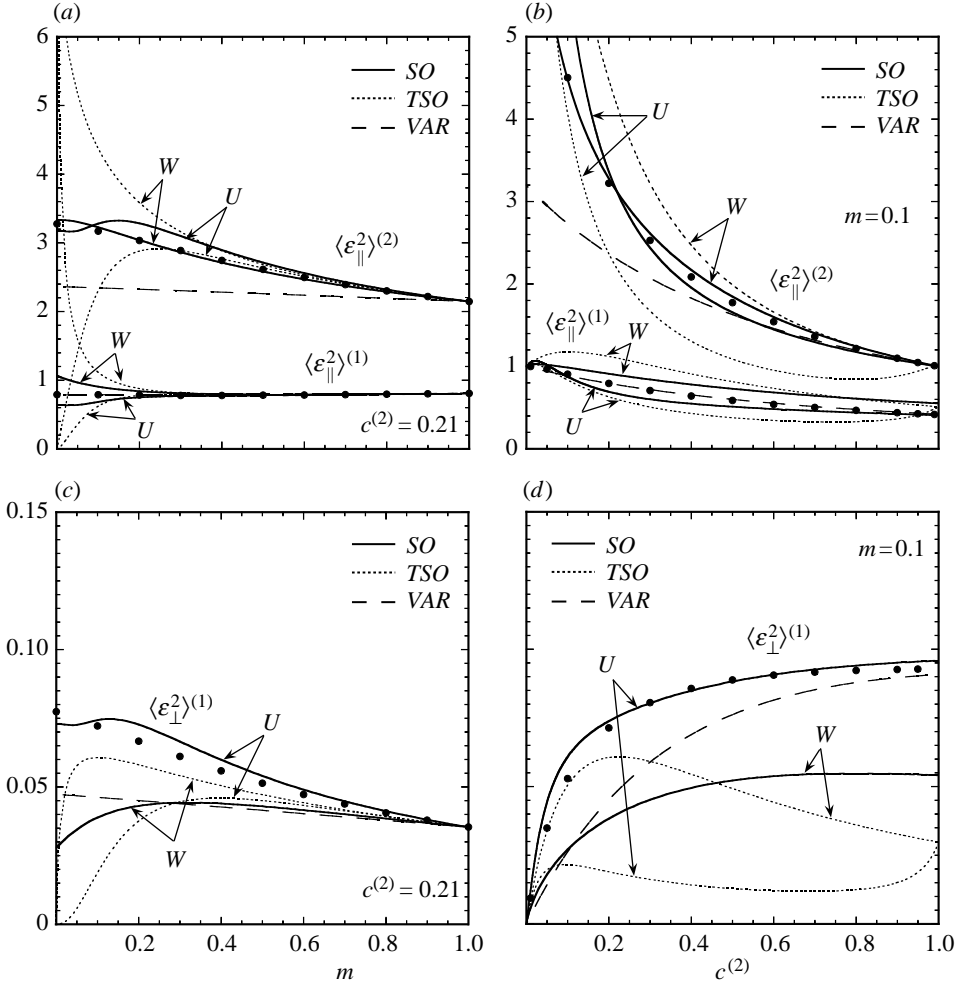


Figure 7. Second moments of the strain field in fibre-weakened composites. ‘Parallel’  $\varepsilon_{\parallel}$  and ‘perpendicular’  $\varepsilon_{\perp}$  components, normalized by  $\bar{\varepsilon}_e^2$ .

general agreement between the exact *LAM* results and the different homogenization estimates is worse than that found for the first moments of the stress (see figure 6c and d), even though the stress statistics are less sensitive than the corresponding strain statistics in the case of weaker fibres. Of all homogenization estimates, the *SO*(*W*) seem to do best for the second moments of the stress, as opposed to the *SO*(*U*) estimates for the corresponding strain quantities, the agreement with the *LAM* results being good for all values of  $m$  and  $c^{(2)}$ . In contrast, both versions of the *TSO* estimates are found to be in good agreement with the *LAM* results for weak-to-moderate nonlinearities, but deteriorate significantly as  $m \rightarrow 0$ , where they violate the inequality  $\langle \sigma_e^2 \rangle^{(2)} \geq (\bar{\sigma}_e^{(2)})^2$ . In particular, the *TSO* estimates for the second moments of  $\sigma_{\perp}$  in the matrix phase are seen to blow up in this limit, which is at odds with the exact *LAM* results.

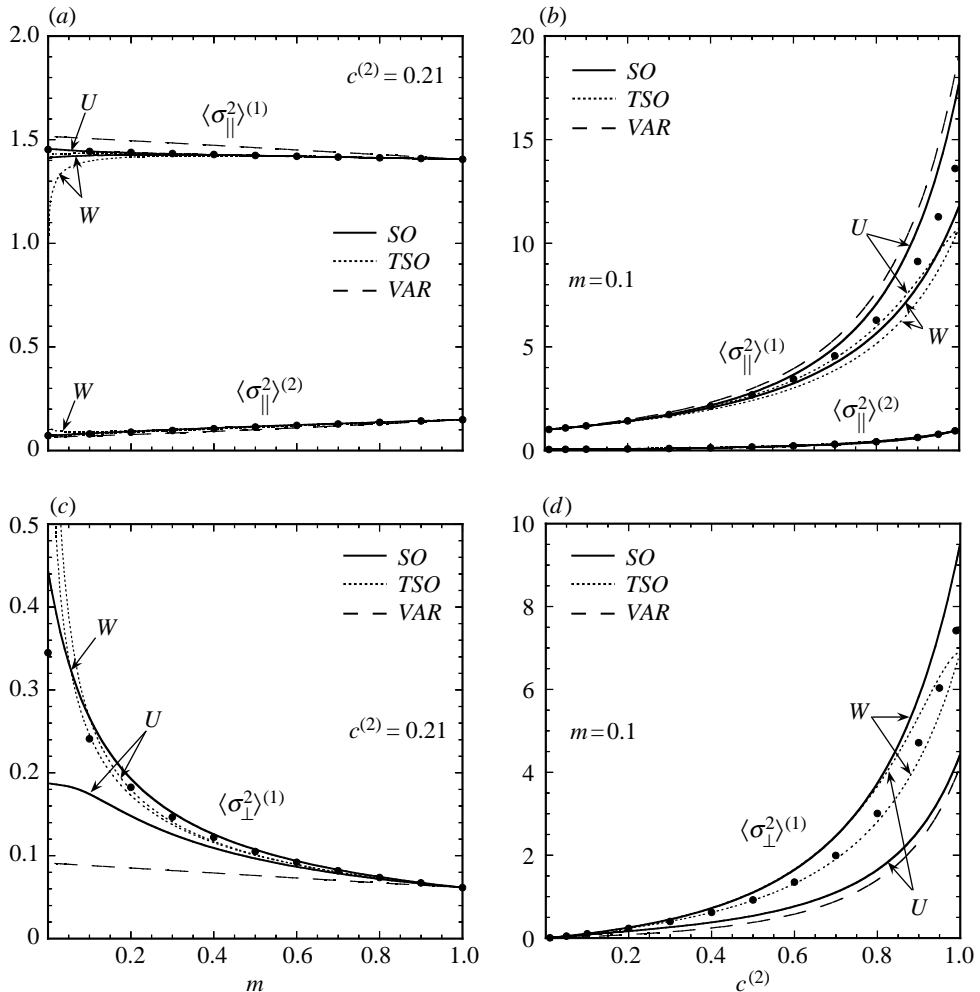


Figure 8. Second moments of the strain field in fibre-weakened composites. ‘Parallel’  $\sigma_{\parallel}$  and ‘perpendicular’  $\sigma_{\perp}$  components, normalized by  $\bar{\sigma}_e^2$ .

Noting that the plots for the stress statistics provided in figures 6 and 8 are appropriately normalized by  $\bar{\sigma}_e$ , which should be set equal to  $\tilde{\sigma}_0$  in the ideally plastic limit for the composite to flow, it is inferred that, as  $m \rightarrow 0$ , the exact LAM results for the second moments of the equivalent stress in the matrix phase  $\sqrt{\langle \sigma_e^2 \rangle^{(1)}}$  tend to the flow stress  $\sigma_0^{(1)}$ , while those for  $\bar{\sigma}_e^{(1)}$  remain below  $\sigma_0^{(1)}$ . In addition, the LAM results for these quantities in the (weaker) inclusion phase tend to the flow stress  $\sigma_0^{(2)}$  in this limit. This means that in ideally plastic, sequential laminates like those considered here, every point is at yield in both phases. However, in the matrix phase, the ‘direction’ of the stress tensor varies with position, thus giving rise to intraphase stress fluctuations even though  $\sigma_e = \sigma_0^{(1)}$  everywhere. This is a very special behaviour that would not be expected to happen in more realistic microstructures, as, for example, in those

considered by Idiart *et al.* (2006). It should be emphasized, nevertheless, that, independently of the microstructure, the stress statistics in ideally plastic composites are such that  $\bar{\sigma}_e^{(r)} \leq \sqrt{\langle \sigma_e^2 \rangle^{(r)}} \leq \sigma_0^{(r)}$ , and therefore accurate estimates should satisfy these inequalities. Even though not shown here (see Idiart (in preparation) for details), it is noted that the *SO* and *VAR* estimates do satisfy these inequalities in the ideally plastic limit, but the *TSO* estimates sometimes violate them. In this connection, it is recalled that the so-called affine method, which amounts to obtaining the estimates directly from the LCC of the *TSO* method and therefore delivers estimates even less accurate than the *TSO* estimates, is already known to predict second moments of the ‘resolved’ shear stresses that are larger than the flow stress of the slip system in the context of viscoplastic polycrystals (see Brenner *et al.* 2004).

## 5. Isotropic, rigidly reinforced composites

In this section, results are provided for the effective behaviour and associated average stresses in isotropic power-law composites with rigid inclusions, subjected to axisymmetric shear ( $\theta=0$ ) and simple shear ( $\theta=\pi/6$ ) loadings. For the sake of brevity, only one value of the strain-rate sensitivity ( $m=0.1$ ) is considered. However, it is worth emphasizing that, while the *TSO* and *SO* estimates for simple shear are found to exhibit a dependence on  $m$  that is similar to that observed in the context of fibre-reinforced composites under in-plane shear, the corresponding estimates for axisymmetric shear predict a reinforcement effect, as well as inhomogeneous stress fields, even in the ideally plastic limit, which seems to be consistent with the exact *LAM* results (*LAM* results could not be obtained for  $m=0$ ).

In figure 9, plots are given for the effective flow stress  $\tilde{\sigma}_0$ , normalized by the flow stress of the matrix  $\sigma_0^{(1)}$ , and the corresponding equivalent average stresses  $\bar{\sigma}_e^{(r)}$ , normalized by the equivalent macroscopic stress  $\bar{\sigma}_e$ , as a function of the reinforcement concentration  $c^{(2)}$ . The main observation in the context of this figure is that, among the nonlinear homogenization estimates for  $\tilde{\sigma}_0$ , the *SO* estimates are found to be the most accurate for all values of the reinforcement concentration under both types of loading conditions considered, as can be seen in figure 9*a,b*. Thus, these estimates predict a lower  $\tilde{\sigma}_0$  in simple shear than in axisymmetric shear loading, in agreement with the trend found for the exact *LAM* results. As for the case of fibre-reinforced composites (see figure 1*b*), it is seen that for low-to-moderate values of  $c^{(2)}$ , the *SO(W)* estimates are closer to the exact *LAM* results than the *SO(U)* estimates, while for large values of  $c^{(2)}$  the converse is true. It can be seen that, while the *TSO* estimates also capture the right dependence on  $\theta$ , they are found to overestimate significantly the exact *LAM* results. The *TSO(U)* estimates for  $\theta=0$  even violate the rigorous bound provided by the *VAR* estimates. Finally, the *VAR* estimates not only overestimate the exact *LAM* results, but also they are unable to capture any dependence on  $\theta$ .

It is recalled that, since the inclusions are rigid, the average strains are trivial in this case, namely  $\bar{\epsilon}^{(2)} = 0$  and  $\bar{\epsilon}^{(1)} = \bar{\epsilon}/c^{(1)}$ . The corresponding average stresses are shown in figure 9*c,d*. It is seen that the *LAM* results exhibit an average stress in the inclusion phase  $\bar{\sigma}_e^{(2)}$  that is larger in axisymmetric shear ( $\theta=0$ ) than in simple shear



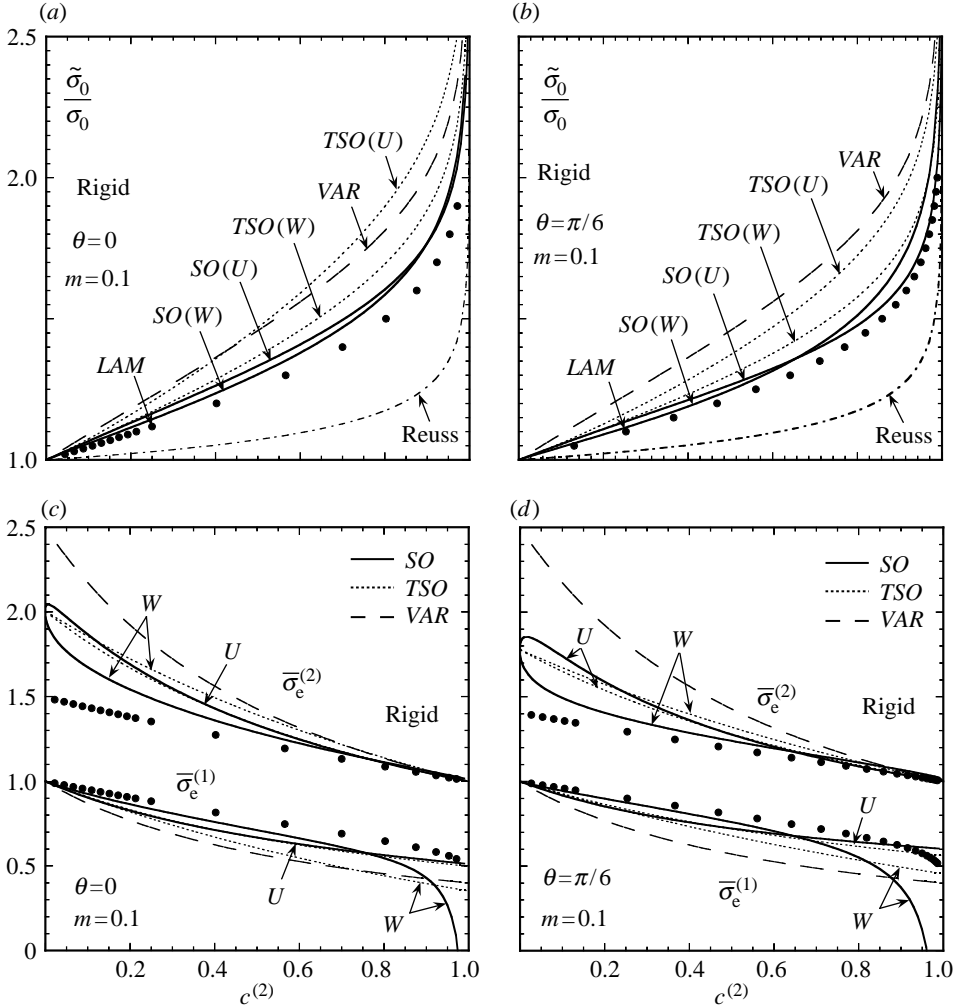


Figure 9. Estimates and exact results for power-law rigidly reinforced composites, as a function of the reinforcement concentration  $c^{(2)}$ , for a given strain-rate sensitivity ( $m=0.1$ ). Effective flow stress  $\tilde{\sigma}_0$ , normalized by the flow stress of the matrix  $\sigma_0^{(1)}$ , for (a) axisymmetric shear ( $\theta=0$ ) and (b) simple shear ( $\theta=\pi/6$ ). Parts (c) and (d) show corresponding equivalent average stresses in each phase  $\bar{\sigma}_e^{(r)}$ , normalized by the equivalent macroscopic stress  $\bar{\sigma}_e$ . Comparisons between the ‘second-order’ ( $SO$ ), ‘tangent second-order’ ( $TSO$ ) and ‘variational’ ( $VAR$ ) estimates of the Hashin–Shtrikman type, and exact results for power-law laminates ( $LAM$ ).

( $\theta=\pi/6$ ), even though the difference is relatively small. The  $SO$  and  $TSO$  estimates are able to capture this dependence on  $\theta$ , unlike the  $VAR$  estimates, but they are seen to overestimate  $\bar{\sigma}_e^{(2)}$  for dilute reinforcement concentrations. Again, it is observed that, for low-to-moderate values of  $c^{(2)}$ , the  $SO(W)$  estimates are in better agreement with the  $LAM$  results than the  $SO(U)$  estimates, while the opposite is true at large  $c^{(2)}$ . In this connection, the  $SO(W)$  estimates for  $\bar{\sigma}_e^{(1)}$  deteriorate significantly as  $c^{(2)} \rightarrow 1$ , as already noted in the case of fibre-reinforced composites. Results for the corresponding second moments of the fields are not given here for brevity, and the reader is referred to Idiart (in preparation).

Finally, it should be mentioned that the ‘optimal’ LCC associated with the  $SO(W)$  estimates for  $\theta=0$  was found to involve an  $\mathbf{L}_0^{(1)}$  that is not strongly elliptic at some moderate values of  $c^{(2)}$ , for small values of  $m$  (smaller than  $m=0.1$ ). The fact that this negative feature is manifested in this ‘extreme’ case is surely related to the non-optimal choice of the reference tensor  $\tilde{\epsilon}^{(1)}$ , which has been set equal to  $\bar{\epsilon}$  in this work (see part I). However, in practice, it does not seem to have a big effect on the predictions for the effective behaviour and phase averages.

## 6. Isotropic porous materials

In this section, results are provided for the effective behaviour and associated average strains in isotropic, ideally plastic ( $m=0$ ) composites with incompressible pores, subjected to axisymmetric shear ( $\theta=0$ ) and simple shear ( $\theta=\pi/6$ ) loadings. In figure 10, plots are given for the effective flow stress  $\tilde{\sigma}_0$ , normalized by the flow stress of the matrix  $\sigma_0^{(1)}$ , as well as for the corresponding equivalent average strains  $\bar{\epsilon}_e^{(r)}$ , normalized by the equivalent macroscopic strain  $\bar{\epsilon}_e$ , as a function of the porosity  $c^{(2)}$ . The main observation in the context of this figure is that both versions of the  $SO$  estimates for the effective flow stress  $\tilde{\sigma}_0$  are in excellent agreement with the exact  $LAM$  results, for all values of the porosity and both types of loading conditions (see figure 10*a,b*), thus capturing the right dependence on  $\theta$ , which happens to be subtle in this case. In contrast, the  $TSO(W)$  estimates for  $\tilde{\sigma}_0$  are found to be accurate for axisymmetric shear, but highly inaccurate for simple shear. In particular, the  $TSO(U)$  estimates are found to coincide with the Voigt upper bound, thus violating the sharper bound provided by the  $VAR$  estimates. On the other hand, the  $VAR$  estimates, even though insensitive to  $\theta$ , are in relatively good agreement with the  $LAM$  results in this case.

It is recalled that, since the inclusions are incompressible pores, the deviatoric parts of the average stresses are trivial in this case, namely  $\bar{\sigma}_d^{(2)} = 0$  and  $\bar{\sigma}_d^{(1)} = \bar{\sigma}_d/c^{(1)}$ . The corresponding average strains are shown in figure 10*c,d*. It is seen that, among the various homogenization estimates, the  $SO$  estimates are in general the most accurate, their agreement with the  $LAM$  results being good for all values of the porosity, under both loading conditions. It is interesting to note that, as  $c^{(2)} \rightarrow 0$ , these estimates predict that the average strain in the pores remains finite in axisymmetric shear (see figure 10*c*), but blow up in simple shear (see figure 10*d*). Even though the available  $LAM$  results are not conclusive in this respect, they strongly suggest that these predictions are indeed correct, which, if true, would constitute a remarkable result. In contrast, the  $TSO(W)$  estimates, while relatively good in axisymmetric shear, become meaningless in simple shear where they predict a zero average strain in the matrix phase. In addition, the  $TSO(U)$  estimates predict a uniform strain field in the composite, i.e.  $\bar{\epsilon}^{(1)} = \bar{\epsilon}^{(2)} = \bar{\epsilon}$ , completely at odds with the exact  $LAM$  results, but consistent with the fact that the corresponding estimates for  $\tilde{\sigma}_0$  coincide with the Voigt bound. Finally, the  $VAR$  estimates are found to underestimate the average strain in the pores for low values of the porosity, and are insensitive to  $\theta$ .

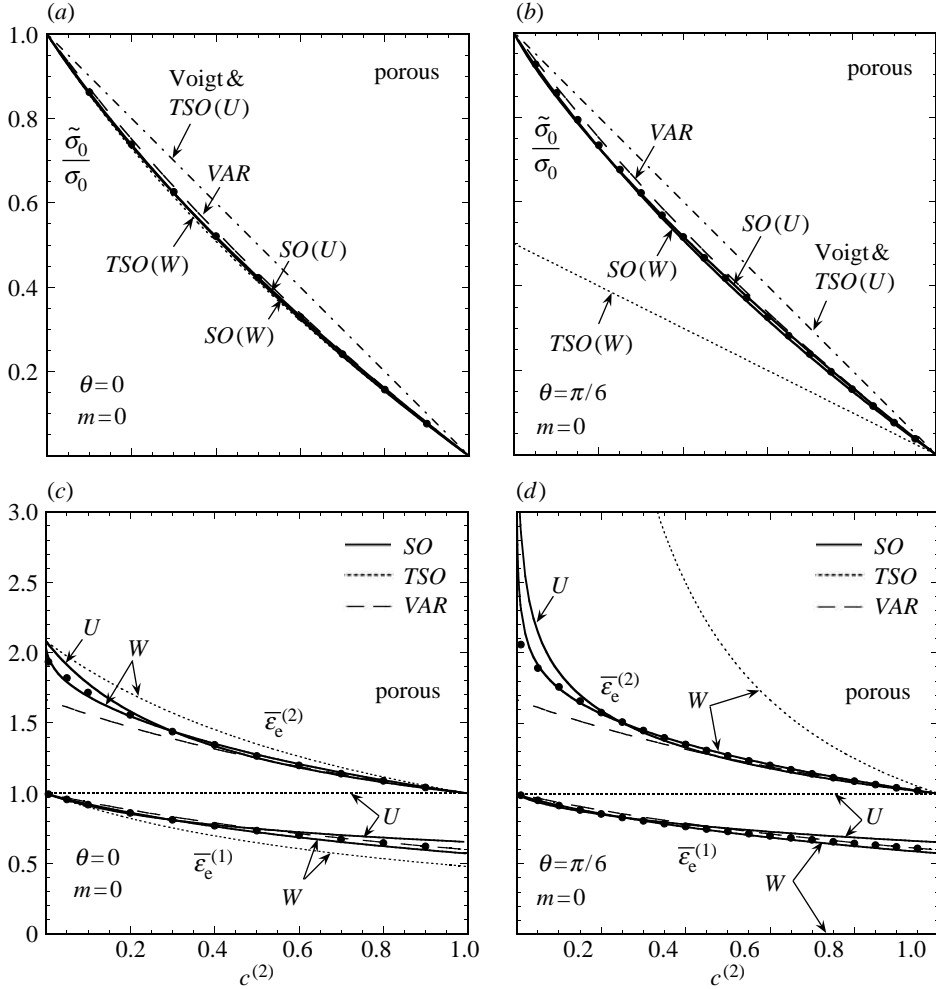


Figure 10. Estimates and exact results for ideally plastic ( $m=0$ ) porous composites, as a function of the porosity  $c^{(2)}$ . Effective flow stress  $\tilde{\sigma}_0$ , normalized by the flow stress of the matrix  $\sigma_0^{(1)}$ , for (a) axisymmetric shear ( $\theta=0$ ) and (b) simple shear ( $\theta=\pi/6$ ). Parts (c) and (d) show corresponding equivalent average strains in each phase  $\bar{\epsilon}_e^{(r)}$ , normalized by the equivalent macroscopic strain  $\bar{\epsilon}_e$ . Comparisons between the ‘second-order’ (SO), ‘tangent second-order’ (TSO) and ‘variational’ (VAR) estimates of the Hashin–Shtrikman type, and exact results for power-law laminates (LAM).

## 7. Concluding remarks

The nonlinear homogenization estimates for the effective behaviour and field statistics proposed in part I of this work have been applied to the specific cases of two-phase, power-law composites with isotropic and transversely isotropic microstructures, and have been compared with available exact results for composites with sequentially laminated microstructures. The main findings are as follows.

Globally, the second-order estimates are found to be superior to the tangent second-order and variational estimates, which can lead to inconsistent predictions in some cases. In particular, the *TSO* estimates have been found to give predictions for the second moments of the stress that are inconsistent with inequalities of the type  $\langle \sigma_e^2 \rangle^{(r)} \geq (\bar{\sigma}_e^{(r)})^2$ , for sufficiently strong nonlinearities.

More specifically, in the case of reinforced composites, both versions of the second-order and tangent second-order estimates for the effective behaviour, as well as for the field statistics, were found to be in fairly good agreement with the exact results for all values of the nonlinearity. All these estimates (*SO* and *TSO*) are able to capture the anisotropic character of the field fluctuations and the fact that certain components of the strain fluctuations in the matrix become unbounded in the strongly nonlinear ideally plastic limit. In contrast, the variational estimates were found to significantly overestimate the effective behaviour, in agreement with their upper bound character, and to give qualitatively incorrect predictions for the field statistics, failing to capture the strong anisotropy of the strain fluctuations at high nonlinearities.

For the cases of fibre-weakened and porous composites, which are more ‘demanding’ than those of reinforced composites, the second-order estimates for the effective behaviour and first moments of the local fields were found to be in good agreement with the exact results even for strong nonlinearities. In general, the accuracy of the corresponding estimates for the second moments of the fields was found to be worse, which is not surprising in view of the fact that they correspond to more sensitive information. However, these estimates agree with the exact results in that, unlike in the case of reinforced composites, the second moments of the strain remain bounded in the ideally plastic limit, thus capturing the relative differences between the deformation patterns in the weaker- and stronger-particle cases. On the other hand, the tangent second-order estimates were found to be fairly accurate for weak-to-moderate nonlinearities, but deteriorate significantly for strong nonlinearities. In turn, the variational estimates were found to be relatively good for the effective behaviour, but qualitatively incorrect for the field statistics.

It is worth mentioning (see Idiart (in preparation) for more details) that accounting for the correction terms derived in part I in the context of the second-order and tangent second-order, estimates for the field statistics always had a beneficial effect, in that they improve the predictions arising from the sole use of the LCC. This improvement can be quite significant at strong nonlinearities, especially for the statistics of the dual field (i.e. the strain statistics arising from the stress formulation of the methods, and vice versa). Finally, it is emphasized that even though the ‘optimal’ choice of the ‘reference tensors’ in the context of the second-order estimates remains an open question, the results provided in this work show that accurate estimates can be obtained by making use of the simplest possible prescriptions for these tensors, namely, the macroscopic fields themselves. In addition, these choices have been shown (see part I) to lead to relatively simple analytical estimates for the first and second moments of the strain and stress fields.

This material is based upon the work supported by the National Science Foundation under Grants CMS-02-01454 and OISE-02-31867.

## References

- Brenner, R., Castelnau, O. & Badea, L. 2004 Mechanical field fluctuations in polycrystals estimated by homogenization techniques. *Proc. R. Soc. A* **460**, 3589–3612. (doi:10.1098/rspa.2004.1278)
- deBotton, G. 2005 Transversely isotropic sequentially laminated composites in finite elasticity. *J. Mech. Phys. Solids* **53**, 1334–1361. (doi:10.1016/j.jmps.2005.01.006)
- deBotton, G. & Hariton, I. 2002 High-rank nonlinear sequentially laminated composites and their possible tendency towards isotropic behavior. *J. Mech. Phys. Solids* **50**, 2577–2595. (doi:10.1016/S0022-5096(02)00049-2)
- Idiart, M. I. In preparation Macroscopic behavior and field fluctuations in viscoplastic composites. Ph.D. thesis, University of Pennsylvania, USA.
- Idiart, M. I. & Ponte Castañeda, P. 2003 Field fluctuations and macroscopic properties in nonlinear composites. *Int. J. Solids Struct.* **40**, 7015–7033. (doi:10.1016/S0020-7683(03)00352-4)
- Idiart, M. I. & Ponte Castañeda P. 2006 Field statistics in nonlinear composites. I. Theory. *Proc. R. Soc. A* **463**, 183–202. (doi:10.1098/rspa.2006.1756)
- Idiart, M. I., Moulinec, H., Ponte Castañeda, P. & Suquet, P. 2006 Macroscopic behavior and field fluctuations in viscoplastic composites: second-order estimates vs full-field simulations. *J. Mech. Phys. Solids* **54**, 1029–1063. (doi:10.1016/j.jmps.2005.11.004)
- Lebensohn, R. A., Liu, Y. & Ponte Castañeda, P. 2004a Macroscopic properties and field fluctuations in model power-law polycrystals: full-field solutions versus self-consistent estimates. *Proc. R. Soc. A* **460**, 1381–1405. (doi:10.1098/rspa.2003.1212)
- Lebensohn, R. A., Liu, Y. & Ponte Castañeda, P. 2004b On the accuracy of the self-consistent approximation for polycrystals: comparison with full-field numerical simulations. *Acta Mat.* **52**, 5347–5361. (doi:10.1016/j.actamat.2004.07.040)
- Liu, Y. & Ponte Castañeda, P. 2004a Second-order theory for the effective behavior and field fluctuations in viscoplastic polycrystals. *J. Mech. Phys. Solids* **52**, 467–495. (doi:10.1016/S0022-5096(03)00078-4)
- Liu, Y. & Ponte Castañeda, P. 2004b Homogenization estimates for the average behavior and field fluctuations in cubic and hexagonal viscoplastic polycrystals. *J. Mech. Phys. Solids* **52**, 1175–1211. (doi:10.1016/j.jmps.2003.08.006)
- Levin, V. M. 1967 Thermal expansion coefficients of heterogeneous materials. *Mekh. Tverd. Tela.* **2**, 83–94.
- Milton, G. W. 2002 *The theory of composites*. Cambridge, UK: Cambridge University Press.
- Moulinec, H. & Suquet, P. 2003 Intraplase strain heterogeneity in nonlinear composites: a computational approach. *Eur. J. Mech. A* **22**, 751–770. (doi:10.1016/S0997-7538(03)00079-2)
- Moulinec, H. & Suquet, P. 2004 Homogenization for nonlinear composites in the light of numerical simulations. In *Nonlinear homogenization and its applications to composites, polycrystals and smart materials* (ed. P. Ponte Castañeda, J. J. Telega & B. Gambin), pp. 193–223. Dordrecht, The Netherlands: Kluwer Academic Publishers.
- Ponte Castañeda, P. 1991 The effective mechanical properties of nonlinear isotropic composites. *J. Mech. Phys. Solids* **39**, 45–71. (doi:10.1016/0022-5096(91)90030-R)
- Ponte Castañeda, P. 1996 Exact second-order estimates for the effective mechanical properties of nonlinear composite materials. *J. Mech. Phys. Solids* **44**, 827–862. (doi:10.1016/0022-5096(96)00015-4)
- Ponte Castañeda, P. 2002a Second-order homogenization estimates for nonlinear composites incorporating field fluctuations: I-theory. *J. Mech. Phys. Solids* **50**, 737–757. (doi:10.1016/S0022-5096(01)00099-0)
- Ponte Castañeda, P. 2002b Second-order homogenization estimates for nonlinear composites incorporating field fluctuations: II-applications. *J. Mech. Phys. Solids* **50**, 759–782. (doi:10.1016/S0022-5096(01)00098-9)
- Willis, J. R. 1981 Variational and related methods for the overall properties of composites. *Adv. App. Mech.* **21**, 1–78.